

# DSLUT: An Asymmetric LUT and its Automatic Design Flow Based on Practical Functions

Moucheng Yang\*, Kaixiang Zhu\*, Lingli Wang\*, and Xuegong Zhou<sup>†</sup>

\*State Key Laboratory of ASIC and System, Fudan University, Shanghai, China

<sup>†</sup>Institute of Big Data, Fudan University, Shanghai, China

<sup>†</sup>zhouxg@fudan.edu.cn

**Abstract**—The conventional LUT is redundant since practical functions in real-world benchmarks only occupy a small proportion of all the functions. For example, there are only 3881 out of more than  $10^{14}$  NPN classes of 6-input functions occurring in the mapped netlists of the VTR8 and Koios benchmarks. Therefore, we propose a novel LUT-like architecture, named DSLUT, with asymmetric inputs and programmable bits to efficiently implement the practical functions in domain-specific benchmarks instead of all the functions. The compact structure of the MUX Tree in the conventional LUT is preserved, while fewer programmable bits are connected to the MUX Tree according to the bit assignment generated by the proposed algorithm. A 6-input DSLUT with 26 SRAM bits is generated for evaluation, which is based on the practical functions of 39 circuits from the VTR8 and Koios benchmarks. After the synthesis flow of ABC, the post-synthesis results show that the proposed DSLUT6 architecture reduces the number of levels by 10.98% at a cost of 7.25% area overhead compared to LUT5 architecture, while LUT6 reduces 15.16% levels at a cost of 51.73% more PLB area. After the full VTR flow, the post-implementation results show that the proposed DSLUT6 can provide performance improvement by 4.59% over LUT5, close to 5.42% of LUT6 over LUT5, causing less area overhead (6.81% of DSLUT6 and 10.93% of LUT6).<sup>1</sup>

## I. INTRODUCTION

Since its first introduction in the 1980s, the field programmable gate array (FPGA) has become an efficient alternative of implementation for digital circuits due to its flexibility and programmability. The SRAM-based look-up table (LUT) used as the programmable logic block (PLB) currently dominates the commercial FPGA architectures because of its complete functionality and EDA friendliness. However, it is quite expensive to raise the number of inputs ( $K$ ) of LUT due to the exponential area growth with  $K$  [1]. On the other hand, the LUT is redundant since practical functions in real-world benchmarks only occupy a small proportion of all the functions. For example, there are only 3881 out of more than  $10^{14}$  NPN classes of 6-input functions in the mapped netlists of the VTR8 [2] and Koios [3] benchmarks.

<sup>1</sup>This work has been accepted for publication in the Proceedings of the International Conference on Field Programmable Technology (ICFPT), 2023. Personal use of this material is permitted. Permission from IEEE must be obtained for all other uses, in any current or future media, including reprinting/republishing this material for advertising or promotional purposes, creating new collective works, for resale or redistribution to servers or lists, or reuse of any copyrighted component of this work in other works.

In order to address the high cost of extension as well as the redundancy of functionality, we propose a novel LUT-like architecture, named DSLUT, with asymmetric inputs and programmable SRAM bits to efficiently implement the practical functions from the domain-specific benchmarks instead of all the functions. Asymmetric inputs prohibit arbitrary input permutation of DSLUT by changing programmable bits, which can be supported by programmable interconnect instead. The compact structure of the MUX Tree in the conventional LUT is preserved, while fewer programmable bits are connected to the MUX Tree according to the bit assignment generated by the proposed algorithm.

In this paper, A 6-input DSLUT with 26 SRAM bits is generated for evaluation, which is based on the practical functions of 39 circuits from the VTR8 and Koios benchmarks. After the synthesis flow of ABC [4], the post-synthesis results show that the proposed DSLUT6 architecture reduces the number of levels by 10.98% at a cost of 7.25% area overhead compared to LUT5 architecture, while LUT6 reduces 15.16% levels at a cost of 51.73% more PLB area. After the full VTR flow [2], the post-implementation results show that the proposed DSLUT6 achieves performance improvement by 4.59% over LUT5, close to 5.42% of LUT6 over LUT5, causing less area overhead (6.81% of DSLUT6 and 10.93% of LUT6). Both of the two experimental results indicate that the proposed DSLUT6 can raise the  $K$  of PLB to improve performance at a lower cost of area.

The major contributions of this paper are listed as follows<sup>2</sup>:

- 1) DSLUT: an asymmetric LUT-like architecture of PLB based on function-distribution analysis of the given benchmarks;
- 2) The generation of DSLUT by a combination of a heuristic algorithm and a hyper-parameter optimization algorithm;
- 3) The SAT-based boolean matching of DSLUT;
- 4) The evaluation by the full EDA flow.

This paper is organized as follows. Section II introduces some previous works and important methods or tools used. Section III describes the proposed DSLUT architecture in detail. Section IV gives experimental results. Section V concludes this paper.

<sup>2</sup><https://github.com/cmy1230/DSLUT.git>

## II. BACKGROUND

### A. Previous Works on Exploration of PLB

In the early years of integrated circuit technology, universal logic modules (ULM) [5] were introduced to facilitate modular synthesis techniques for logic networks, which can realize all the possible functions of a given number of inputs. For example, [6] designed a 5-input ULM by enumerating all the 3-input NPN classes, which can realize all the 3-input functions. However, the ULM required 36 inputs to implement all the 6-input functions [7]. In order to reduce the number of I/O terminals, the prototype of LUT, called serially controlled ULM then, was first proposed in [8], whose 64 inputs were driven by constant 0 or 1 from internal shift registers and other 6 inputs by external I/O terminals.

Many research efforts are devoted to improving the logic density and area efficiency of LUT. An extended LUT which contains a LUT and several logic gates is proposed in [9] to raise the functionality. These two papers [10] and [11] both evaluate several generic LUT-based PLB architectures which consist of interconnected LUTs and logic gates.

On the other hand, several non-LUT-like PLBs such as [12] and [13] are designed by investigating the most frequently used functions in standard benchmarks. However, only 4-input functions are considered due to the limitation of manual design. In this paper, an automatic design flow is proposed to generate DSLUT by investigating functions with 6 or more inputs.

Commercial FPGAs have different PLBs to raise area efficiency. The PLB proposed in [14] consists of MUX4 and two logic gates connected. The Stratix 10 ALM [15] has a fracturable PLB with 8 independent inputs which can implement two 5-input functions sharing 8 inputs or any 6-input functions. In Versal architecture from Xilinx [16], the LUT is enhanced to increase effective packing density and functionality so that two independent functions of up to 6 unique inputs can be packed in one PLB.

### B. Classification of Logic Function by NPN

Logic function classification is the problem of grouping functions into equivalence classes. The most frequently used classification method is based on Negation-Permutation-Negation (NPN) equivalence. Two Boolean functions are NPN equivalent, if one can be obtained from the other by negating inputs, permuting inputs, and negating the output.

In this paper, fast exact NPN classification [17] is used to dramatically reduce complexities in function enumeration, generation of the function library, and boolean matching in technology mapping. The number of NPN classes of functions with different numbers of inputs is shown in Table I, where the NPN capacity is the maximum number of functions an NPN class can contain, and  $nPracticalClass$  is the number of the practical NPN classes in mapped netlists of VTR8 and Koios benchmarks.

TABLE I  
THE NUMBER OF NPN CLASSES

nInputs	nFuncs	NPN capacity	nAllClass	nPracticalClass
K	$2^{(2^K)}$	$2^{(k+1)} * k!$		
2	16	8	4	4
3	256	48	14	10
4	65536	768	222	150
5	$4.3 \times 10^9$	7680	616126	1026
6	$1.8 \times 10^{19}$	92160	$\sim 10^{14}$	3881
7	$3.4 \times 10^{38}$	1290240	$\sim 10^{32}$	7843
8	$1.2 \times 10^{77}$	$2 \times 10^7$	$\sim 10^{69}$	14309

### C. Boolean Matching for General PLB

If a PLB with incomplete functionality instead of the standard LUT is used in the FPGA, boolean matching has to be involved in the technology mapping flow, to determine whether a function can be implemented by the given PLB. There are three existing methods of boolean matching for FPGAs: function decomposition [10], the pre-computed library [14], and boolean satisfiability [11]. The method based on function decomposition is fast but inflexible because a new boolean matching algorithm has to be designed for each new PLB. The method based on the pre-computed library has a high space complexity when the number of inputs is greater than 5 because all the functions that can be implemented by the given PLB are enumerated. The last SAT-based method is general for any PLBs, but very time-consuming.

In this paper, we use an integrated SAT-based approach based on a pre-computed practical function library, which is similar to [18], to map logic netlists into arbitrary single-output PLBs. In order to accelerate the SAT solving, the well-known paradigm of counterexample guided abstraction refinement (CEGAR) [19] is applied. The boolean matching in [18] only supports coarse-grained PLBs containing LUTs, MUXes, and elementary 2-input logic gates, while the SAT-based boolean matching implemented by us in Python is able to support fine-grained DSLUT.

### D. Automatic Hyper-parameter Optimization

The generation of DSLUT can be formulated as a problem of hyper-parameter optimization, whose target is to maximize the coverage of a given DSLUT with the given number of SRAM bits. A meta-modeling approach to support automated hyper-parameter optimization is proposed in [20], which has an open-source package of Python named *hyperopt*.

There are four important components of *hyperopt*: the objective function to minimize, the space over which to search, the search algorithm to use, and the database in which to store all the point evaluations of the search. After the definitions of these four components, *hyperopt* can find the best value of the scalar-valued, possibly-stochastic objective function over a set of possible arguments to that function.

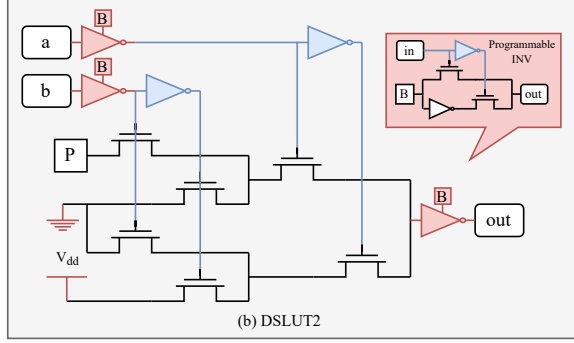
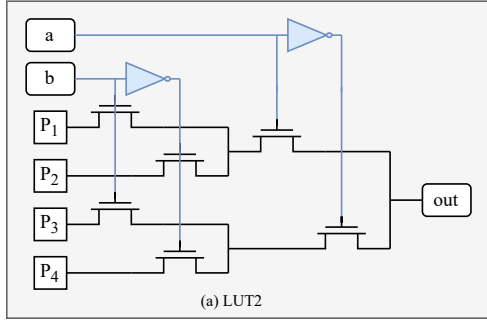


Fig. 1. LUT2 and DSLUT2

### III. PROPOSED ARCHITECTURE

#### A. DSLUT: Domain-Specific LUT

In order to introduce the DSLUT, we first take LUT2 and DSLUT2 as examples, as shown in Fig.1. LUT2 can be seen as a ULM6, whose function  $G$  is formulated as equation 1.  $\{P_i\}$  are four programmable SRAM bits, while  $a$  and  $b$  are two inputs. After  $\{P_i\}$  is given, the function  $G$  of LUT2 is then determined. There are 16 2-input functions in total, taking 4 bits to encode. However, if function classification by NPN is concerned, there are only 4 classes of 2-input functions, taking fewer bits to encode.

$$G(a, b, P_1, P_2, P_3, P_4) = \bar{a}\bar{b}P_1 + a\bar{b}P_2 + \bar{a}bP_3 + abP_4 \quad (1)$$

As shown in Fig.1.(b), three programmable inverters ( $PINV$ ) are added to I/O terminals so that operations of I/O negation are supported. Therefore, we only need to consider one function for each NPN class. For example, we consider two function:  $G(a, b, 0, 0, 0, 1) = ab$  and  $G(a, b, 1, 0, 0, 1) = ab + \bar{a}\bar{b}$  representing two 2-input NPN classes. Only one programmable bit is required to encode these two NPN classes, that is  $G(a, b, P, 0, 0, 1) = H(a, b, P) = ab + P\bar{a}\bar{b}$ , as shown in Fig.1.(b). Single-input and constant functions can be realized by bridging inputs, such as  $H(a, a, 0) = a$  and  $H(a, \bar{a}, 0) = 0$ . So far, we still use four SRAM bits (the  $PINV$  takes one SRAM bit each) to encode four 2-input NPN classes. When the  $K$  of DSLUT is increased, the reduction in the number

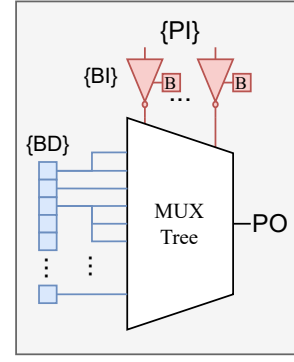


Fig. 2. Schematic of DSLUT

of SRAM bits comes from 1) asymmetry of inputs; 2) input bridging, and 3) limited coverage of NPN classes.

Now we introduce the proposed asymmetric LUT-like PLB named DSLUT, as shown in Fig.2, where the compact structure of the MUX tree is preserved.  $\{B_D\}$  are the actual existing SRAM bits. The connection pattern between  $\{B_D\}$  and the data inputs of the MUX tree is called bit assignments. In order to decrease the delay overhead, the  $PINV$  added to the output is removed. Therefore, the data input of the MUX tree cannot be driven by constant 0 or 1 so as to support output negation. Once the number of SRAM bits in  $\{B_D\}$  and the bit assignment are fixed, the function of the DSLUT is determined.

#### B. Library of Practical Functions

Since the algorithm of technology mapping, named as *if* in ABC [4], includes the stage of cut enumeration [21], it can be used to build a function library by harvesting functions in the given benchmarks. A novel representation of boolean functions in terms of their disjoint-support decomposition (DSD) [22] is used to make the function library more compact, because it is equivalent to NPN classification and supports fine-grained structure hashing.

Besides used for boolean matching as mentioned in Section II-C, the function library with additional statistical information can give an insight into function distribution. We define three kinds of occurrence of a function:  $nOccurEnum$ ,  $nOccurCutset$  and  $nOccurCutBest$ . For each function in the function library, its  $nOccurEnum$  will count when it is enumerated in cut enumeration. Its  $nOccurCutset$  will count when it is included in the cut set of an AIG node in *If*, while its  $nOccurCutBest$  will count when it is selected as a LUT in the mapped netlist.

Occurrence counting is added into generation of the function library in *if*. Occurrence rates are computed by dividing the  $nOccurCutBest$  of a function by the sum of  $nOccurCutBests$  of all the functions. The occurrence rates of the top20 6-input functions in VTR8 and Koios benchmarks are shown in Fig.3, which shows that the top 5% (20 out of 3881) of 6-input functions account for 80% of  $nOccurCutBests$  of all functions.

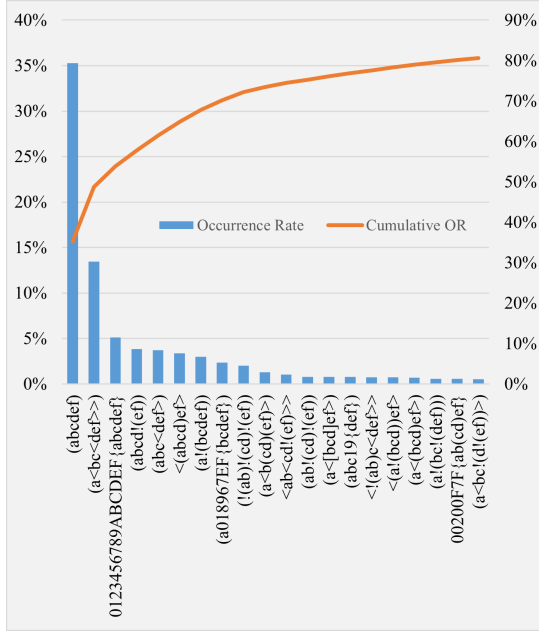


Fig. 3. Occurrence Rates of the TOP20 6-input Functions in VTR8 and Koios Benchmarks

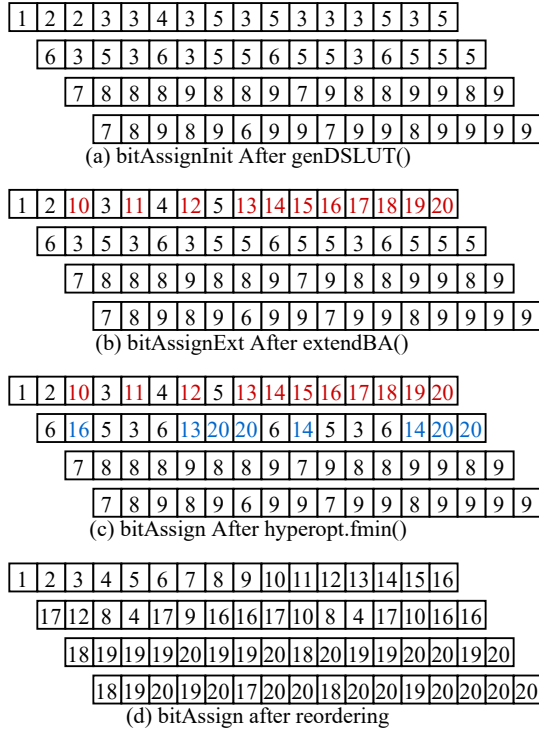


Fig. 4. An Example of Bit Assignment

The definition of expressions for boolean functions can be found in [22].

#### Algo 1: The pseudo-code of DSLUT generation

```

Input : nInputs, funcLib.dsd
Output: bitAssign
1 funcLib ← loadLib("funcLib.dsd");
2 funcList ← [f for f in funcLib if f.nvars == nInputs];
3 funcList ← sortByOccurrence(funcList);
4 numTopFuncs ← 8; //Predetermined
5 ttList ← list(); //tt means truthTable
6 for i ← 0 to (numTopFuncs - 1) do
7   func ← funcList[i];
8   if i == 0 then
9     ttList.append(func.getTt());
10  else
11    ttCandidates ← enumTtByNPN(func);
12    for tt in ttCandidates do
13      ttList.append(tt);
14      cost ← computeCost(ttList);
15      if cost < costMin then
16        costMin ← cost;
17        ttBest ← tt;
18      ttList.remove(tt);
19    end
20    ttList.append(ttBest);
21  end
22 end
23 bitAssignInit ← genDslut(ttList);
24 bitAssignExt, bitMap ← extendBA(bitAssignInit);
  /*obj computes the coverage rate of a
    DSLUT by boolean matching */
25 obj: bitAssign, funcList → coverage;
26 space ← genSpace(bitAssignExt, bitMap);
27 algo ← mixSuggest((0.25,rand), (0.75,tpe));
28 bitAssign ← hyperopt.fmin(obj, space, algo);

```

#### C. Generation of Bit Assignments

The generation of bit assignments of a DSLUT is shown in Algorithm 1, which consists of two major stages: a heuristic algorithm for initialization and the hyper-parameter optimization by *hyperopt*. Theorem 2.2.1 in [23] implies that a DSLUT with a given bit assignment can implement a function, if and only if for any two positions whose bits are different in the truth table of the function, the corresponding driving bits in  $\{B_D\}$  according to the bit assignment are different.

Taking DSLUT2 shown in Fig.1.(b) as example, the bit assignment  $\{P_1, P_2, P_2, P_2\}$ , resulting in  $G(a, b, P_1, P_2, P_2, P_2)$  can implement the function  $f$  with truth table (1,0,0,0), while the bit assignment  $\{P_1, P_1, P_2, P_2\}$  can not. The reason is that the first two bits of the latter bit assignment are the same, while the first two bits of the truth table of  $f$  are different, which makes it impossible to implement the function.

Due to the additional PINVs, only one function of a NPN class needs to be considered. We can enumerate all the functions belonging to an NPN class to find the proper function

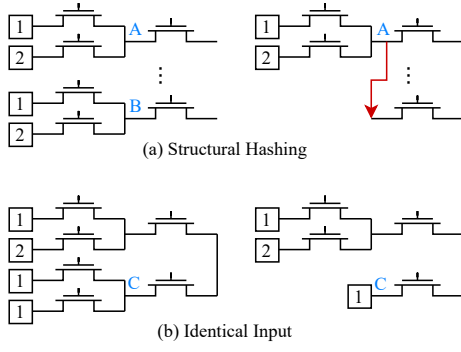


Fig. 5. Two Situations of MUX Tree Optimization

as the representative, as shown in line 6 to line 22 in Algorithm 1. The minimum number of bits in the bit assignment for the given functions is computed in the function *computeCost()* in line 14.

In order to be compatible with LUT for small functions, the first 16 bits in the bit assignment are extended to be different from each other, resulting in a LUT4, as shown in line 24, while the changes caused by the extension are stored in *bitMap*. New differences between bits in the bit assignment are introduced by *hyperopt* within the limit of *bitMap* to preserve the previous differences.

The bit assignments in different stages of the generation of the proposed DSLUT6 are shown in Fig.4 as an example.

#### D. Optimization of the MUX Tree

Since the data inputs of the MUX tree are driven by fewer SRAM bits, the MUX tree itself can be optimized. There are two situations where the transistors in the MUX tree can be pruned, which are called structural hashing and identical inputs, as shown in Fig.5.

It is worth noting that when the transistors are removed due to identical inputs, as shown in Fig.5.(b), the delay between the removed input and the output in the optimized data path is reduced to zero, which will reduce the average delay of all the data paths of all the inputs.

#### E. Delay and Area Modeling

The MUX tree and the bit assignment of the proposed DSLUT6 to be evaluated in Section IV is shown in Fig.6. 18 transistors are pruned due to identical inputs, while 14 transistors are pruned due to structural hashing. There are 94 transistors in the MUX tree of DSLUT6, while 62 and 126 transistors in the MUX tree of LUT5 and LUT6 respectively.

Since the DSLUT is quite similar to the LUT, the area models are based on the modeling results of fracturable LUT5 and LUT6 in 22nm from COFFE [24], as shown in Table II, while the delay model is based on the delays in architecture description file *k6\_frac\_N10\_frac\_chain\_mem32k\_40nm.xml*, which is used as the baseline architecture.

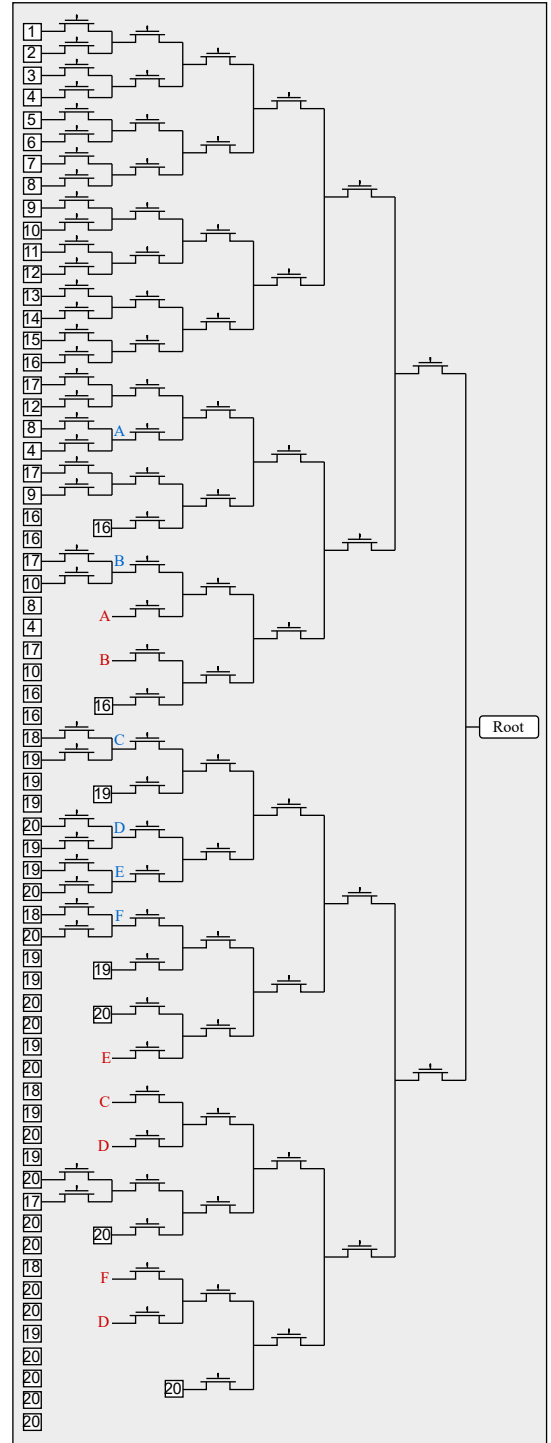


Fig. 6. MUX tree of the Proposed DSLUT6 with a given bit assignment

As shown in Fig.7, the *PINVs* added to the inputs of DSLUT6 cause the area overhead of 4 pass transistors and one SRAM bit. The *other buffer* in Table II includes internal buffers and output buffers. The DSLUT6 is divided into two LUT3 in the fractured mode so that the output buffers are replaced by the internal buffers. Therefore, the area of the *other buffer* is smaller than LUT5 and LUT6.

TABLE II  
MODELING OF DSLUT6 BASED ON COFFE [24] IN 22NM

PLB area ( $\mu m^2$ )	LUT5	DSLUT6	LUT6
numSRAM	32	26	64
total SRAM	6.702	5.445	13.404
MUX tree	3.747	5.799	7.481
input buffer	2.901	4.730	3.525
other buffer	3.555	2.828	3.751
total PLB	16.905	18.802	28.161

CLB area ( $\mu m^2$ )	LUT5	DSLUT6	LUT6
10 PLB	169.049	188.024	281.608
10 FF	10.458	10.458	10.458
crossbar	203.063	243.675	243.675
out mux	21.872	21.872	21.872
carry	44.856	44.856	44.856
total CLB	449.298	510.066	602.469

delay (ps)	LUT5	DSLUT6	LUT6
input[0]	82	102	82
input[1]	173	193	173
input[2]	261	281	261
input[3]	263	283	263
input[4]	398	417	397
input[5]	N/A	418	398
average	235.40	282.17	262.33

Furthermore, the difference in delay between DSLUT and LUT primarily stems from the additional PINVs added to the inputs. The delay overhead caused by the PINVs separately in the COFFE, which is 19.84ps, same as a 2-to-1 multiplexer with two inverters. Because VPR cannot support LUT rebalancing, the average of the delays of the LUTs or DSLUTs from all the inputs to the output is taken as the equivalent delay to get more stable results.

#### IV. EXPERIMENTAL RESULTS

##### A. Experimental Methodology

In order to demonstrate that the proposed DSLUT can extend the K of PLB to improve performance causing less area overhead than that of the LUT architecture, 39 benchmark circuits are synthesized and implemented in three PLB architectures including LUT5, DSLUT6 and LUT6, which share the same routing architecture.

At first, the function coverage of the proposed DSLUT6 is to be evaluated. Then, the post-synthesis results of the ABC flow and the post-implementation results of the full VTR flow are discussed separately. The delays and areas of each architecture are averaged across all benchmark circuits, using the geometric average. The geometric average delay and area of each architecture is normalized to the LUT5 architecture for comparison.

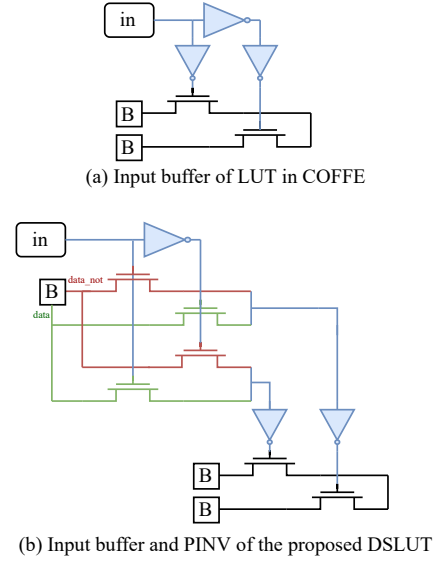


Fig. 7. The Input Buffer and Programmable INV

##### B. Experimental Setups

1) *Benchmarks*: 39 circuits from the VTR8 [2] and Koios [3] benchmark sets are used for the generation of the practical-function library and the architecture evaluations.

2) *EDA Flow*: As shown in Fig.8, the EDA flow is divided into two major parts: the offline flow and the online flow. In the offline flow, the function library is built for boolean matching and DSLUT generation. In the online flow, the delay, and area information by PLB modeling is added to the architecture file first. When technology mapping, the function library and the matching results are loaded into ABC by corresponding instructions. Note that the instruction named *load\_mr* is added by us specifically for the DSLUT.

3) *Baseline Architectures*: The existing architecture file named *k6\_frac\_N10\_frac\_chain\_mem32k\_40nm.xml*, which is included in the VTR directory, is used as the baseline architecture, with all the architectural parameters preserved for the LUT6 architecture to evaluate. For the LUT5 architecture, the PLB is replaced with a fracturable LUT5. For the DSLUT6 architecture, the PLB is replaced with the proposed DSLUT6, which can be fractured to two LUT3s. Since VPR cannot do LUT rebalancing, the average of the delays from all the inputs to the output is taken as the identical delays of inputs to get more stable results. The areas of the different PLBs and CLBs are shown in Table II. Moreover, the channel width of all the three architectures is 300.

##### C. Coverage of Practical Functions

As shown in Table III, the proposed DSLUT6 can realize 780 out of 3881 NPN classes of 6-input practical functions in the library, using only 26 SRAM bits.



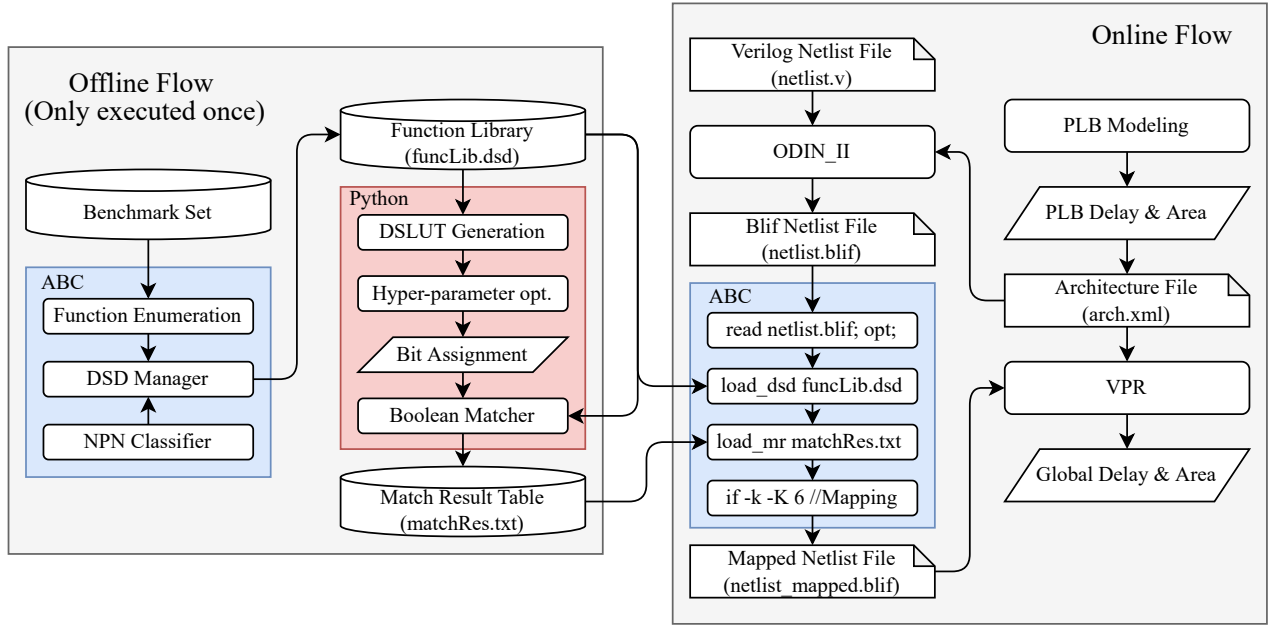


Fig. 8. Full EDA Flow

TABLE III  
THE COVERAGE OF THE PROPOSED DSLUT6

nInputs	numClass
3	10/10
4	150/150
5	910/1026
6	780/3881

#### D. Post-Synthesis Results

After the ABC flow, the detailed post-synthesis results of 39 benchmark circuits are shown in Table IV. The *maxLevel* is the maximum number of PLBs in the critical path of the combinational parts of the benchmark circuit. The *area* is computed by multiplying the *nPLB* by the PLB area shown in Table II. The fracturability of the PLB is not taken into consideration.

The post-synthesis results show that the proposed DSLUT6 architecture reduces the number of levels by 10.98% at a cost of 7.25% area overhead compared to LUT5 architecture, while LUT6 reduces 15.16% levels at a cost of 51.73% more PLB area. In addition, the DSLUT6 architecture has the minimum delay-area product.

#### E. Post-implementation Results

After the full VTR flow, the detailed post-implementation results of 39 benchmark circuits are shown in Table V. The *delay* is extracted directly from the result file *vpr.out*, while the *area* is the product of the *nCLB* and the CLB area shown in Table II. The area of the routing architecture is not considered since it is difficult to quantify the utilization of routing resources.

The post-implementation results show that the proposed DSLUT6 can provide performance improvement by 4.59% over LUT5, close to 5.42% of LUT6 over LUT5, causing less logic area overhead (6.81% of DSLUT6 and 10.93% of LUT6). The delay-area product of the DSLUT6 architecture is better than that of the LUT6 architecture.

#### V. CONCLUSION

An asymmetric LUT-like PLB architecture named DSLUT and its automatic design flow are proposed to address the high cost of extension as well as the redundancy of functionality in the conventional LUT. A library of practical functions harvested from a given benchmark set is built for the analysis of the functional distribution and boolean matching. An algorithm combining a heuristic initialization and hyper-parameter optimization is proposed to generate the bit assignment of DSLUT on the basis of the function library.

The experimental results show that the proposed DSLUT6 containing 26 SRAM bits can implement 780 out of 3881 practical functions. Moreover, the FPGA architecture using DSLUT6 as PLB can achieve better performance by extending the *K* of PLB with less logic area overhead.

#### REFERENCES

- [1] J. Rose, A. El Gamal, and A. Vincentelli, "Architecture of field-programmable gate arrays," *Proceedings of the IEEE*, vol. 81, pp. 1013 – 1029, 08 1993.
- [2] K. E. Murray, O. Petelin, S. Zhong, J. M. Wang, M. Eldafrawy, J.-P. Legault, E. Sha, A. G. Graham, J. Wu, M. J. P. Walker, H. Zeng, P. Patros, J. Luu, K. B. Kent, and V. Betz, "Vtr 8: High-performance cad and customizable fpga architecture modelling," *ACM Trans. Reconfigurable Technol. Syst.*, vol. 13, no. 2, jun 2020. [Online]. Available: <https://doi.org/10.1145/3388617>

TABLE IV  
POST-SYNTHESIS RESULTS

netlist	LUT5			DSLUT6			LUT6		
	maxLevel	nPLB	area ( $\mu m^2$ )	maxLevel	nPLB	area ( $\mu m^2$ )	maxLevel	nPLB	area ( $\mu m^2$ )
arm_core	23	15066	254691	19	14602	274547	19	13695	385665
attention_layer	9	22264	376373	8	21965	412986	7	21740	612220
bgm	25	56194	949960	21	54833	1030970	21	46738	1316189
blob_merge	6	7964	134631	6	7654	143911	5	7227	203520
bnn	3	82217	1389878	3	82086	1543381	3	82134	2312976
boundtop	12	3312	55989	9	3119	58643	10	2982	83976
clstm_like.large	5	864599	14616046	4	849469	15971716	4	831080	23404044
clstm_like.medium	5	585804	9903017	4	576274	10835104	4	563577	15870892
clstm_like.small	5	306707	5184882	4	302644	5690312	4	296007	8335853
conv_layer	5	26061	440561	5	25872	486445	4	25514	718500
conv_layer_hls	8	9976	168644	8	9291	174689	7	9410	264995
dla_like.medium	6	278077	4700892	5	276927	5206781	5	268297	7555512
dla_like.small	6	117242	1981976	5	115531	2172214	5	111169	3130630
eltwise_layer	6	15556	262974	5	14888	279924	5	14528	409123
gemm_layer	10	424464	7175564	9	386424	7265544	9	372094	10478559
lstm	8	106762	1804812	7	106312	1998878	7	105829	2980250
LU32PEEng	129	97424	1646953	113	90927	1709609	108	84037	2366566
LU64PEEng	131	188219	3181842	112	174859	3287699	109	161835	4557435
LU8PEEng	130	28827	487320	113	27351	514254	107	25443	716500
mcml	32	105205	1778491	27	104012	1955634	26	101070	2846232
mkDelayWorker32B	9	6473	109426	8	6103	114749	7	5992	168741
mkPktMerge	3	389	6576	3	387	7276	3	381	10729
mkSMAAdapter4B	6	2352	39761	6	2246	42229	5	2078	58519
or1200	10	3362	56835	8	3072	57760	8	2791	78597
raygentop	4	2566	43378	4	2474	46516	4	2292	64545
reduction_layer	7	11979	202505	6	12101	227523	6	9097	256181
robot_rl	17	22996	388747	15	21705	408097	14	20701	582961
sha	4	2094	35399	3	2506	47118	3	1620	45621
softmax	12	23733	401206	10	21470	403679	10	20975	590677
spmv	8	7138	120668	7	6179	116178	6	5732	161419
spree	19	1055	17835	16	1021	19197	15	931	26218
stereovision0	6	14365	242840	6	14344	269696	5	14152	398534
stereovision1	3	13114	221692	3	12601	236924	3	12490	351731
stereovision2	3	19452	328836	3	19402	364796	3	19391	546070
stereovision3	5	242	4091	5	225	4230	4	208	5857
tiny_darknet_like.medium	8	292287	4941112	8	274039	5152481	7	266097	7493558
tiny_darknet_like.small	8	102991	1741063	7	92378	1736891	7	89027	2507089
tpu_like.medium	6	105025	1775448	5	97872	1840189	5	97656	2750091
tpu_like.small	5	27147	458920	5	26867	505153	5	26470	745422
geomean	9.043	24140.78	408100.0	8.050	23279.44	437700.1	7.672	21987.79	619198.1
percentage	100%	100%	100%	89.02%	96.43%	107.25%	84.84%	91.08%	151.73%
delay-area product	3690560	100%		3523559	95.47%		4750744	128.73%	

TABLE V  
POST-IMPLEMENTATION RESULTS: CRITICAL PATH DELAY AND LOGIC AREA

netlist	LUT5			DSLUT6			LUT6		
	delay (ns)	nCLB	area ( $\mu m^2$ )	delay (ns)	nCLB	area ( $\mu m^2$ )	delay (ns)	nCLB	area ( $\mu m^2$ )
arm_core	19.774	1332	598464.9	20.024	1172	596413.2	19.035	1094	659101.1
attention_layer	9.026	1715	770546.1	8.724	1586	807091.6	8.255	1489	897076.3
bgm	27.434	5055	2271201.4	27.509	5278	2685895.0	26.552	4355	2623752.5
blob_merge	15.922	707	317653.7	14.330	663	337390.8	14.835	618	372325.8
bnn	8.776	7514	3376025.2	8.850	6411	3262461.7	9.591	6382	3844957.2
boundtop	8.254	278	124904.8	6.901	272	138416.7	7.413	244	147002.4
clstm_like.large	19.074	82231	36946223.8	20.162	76863	39114427.8	15.478	60379	36376475.8
clstm_like.medium	20.548	55337	24862803.4	14.737	51882	26401971.6	13.449	40766	24560251.3
clstm_like.small	12.972	28582	12841835.4	10.624	26911	13694604.2	9.506	21172	12755473.7
conv_layer	5.907	2174	976773.9	5.640	1962	998432.4	6.224	1806	1088059.0
conv_layer_hls	14.343	2157	969135.8	13.928	2069	1052883.1	13.640	1998	1203733.1
dla_like.medium	9.811	18754	8426134.7	9.448	18266	9295293.4	10.349	17385	10473923.6
dla_like.small	8.850	8145	3659532.2	10.461	8058	4100595.3	9.092	7579	4566112.6
eltwise_layer	5.415	1245	559376.0	5.076	1209	615242.0	5.432	1098	661511.0
gemm_layer	16.011	38540	17315944.9	14.450	35527	18079157.4	15.796	31818	19169358.6
lstm	9.100	8481	3810496.3	9.398	6850	3485862.3	9.382	6364	3834112.7
LU32PEEng	88.817	8873	3986621.2	79.887	8466	4308220.4	80.329	7610	4584789.1
LU64PEEng	87.064	17140	7700967.7	78.800	16188	8237830.4	80.517	14649	8825568.4
LU8PEEng	88.325	2625	1179407.3	83.682	2508	1276283.6	81.947	2254	1357965.1
mcml	49.664	9617	4320898.9	40.374	9413	4790134.5	42.781	6870	4138962.0
mkDelayWorker32B	8.687	569	255650.6	8.591	550	279886.8	8.776	524	315693.8
mkPktMerge	4.088	28	12580.3	3.775	22	11195.5	4.202	21	12651.8
mkSMAAdapter4B	6.292	238	106932.9	6.049	224	113990.2	5.431	204	122903.7
or1200	8.482	323	145123.3	8.302	300	152665.5	8.718	267	160859.2
raygentop	5.159	225	101092.1	4.933	226	115008.0	4.732	183	110251.8
reduction_layer	7.455	1197	537809.7	7.452	1272	647301.7	6.705	986	594034.4
robot_rl	11.516	1968	884218.5	11.032	1951	992834.6	11.142	1617	974192.4
sha	10.587	215	96599.1	10.180	259	131801.2	9.829	166	100009.9
softmax	10.795	1718	771894.0	9.174	1662	845766.9	9.640	1403	845264.0
spmv	6.769	846	380106.1	6.907	679	345532.9	6.987	620	373530.8
spree	11.315	97	43581.9	12.439	90	45799.7	10.957	73	43980.2
stereovision0	3.834	840	377410.3	3.857	829	421865.7	3.555	801	482577.7
stereovision1	5.490	904	406165.4	5.374	824	419321.2	5.417	796	479565.3
stereovision2	15.592	1828	821316.7	15.291	1670	849838.0	15.109	1660	1000098.5
stereovision3	2.665	20	8986.0	2.785	20	10177.7	2.592	13	7832.1
tiny_darknet_like.medium	20.333	27178	12211021.0	16.854	24268	12349621.2	18.916	22143	13340471.1
tiny_darknet_like.small	19.760	9986	4486689.8	20.112	8706	4430352.8	21.383	8030	4837826.1
tpu_like.medium	10.486	6559	2946945.6	10.220	6068	3087914.2	10.411	5639	3397322.7
tpu_like.small	7.660	1773	796605.4	7.666	1789	910395.3	7.400	1590	957925.7
geomean	11.987	2108	947145.5	11.436	1988	1011654.6	11.337	1744	1050633.7
percentage	100%	100%	100%	95.41%	94.30%	106.81%	94.58%	82.72%	110.93%
delay-area product	11353015.9	100%		11569750	101.91%		11911261	104.92%	



- [3] A. Arora, A. Boutros, D. Rauch, A. Rajen, A. Borda, S. A. Damghani, S. Mehta, S. Kate, P. Patel, K. B. Kent, V. Betz, and L. K. John, "Koios: A deep learning benchmark suite for fpga architecture and cad research," in *2021 31st International Conference on Field-Programmable Logic and Applications (FPL)*, 2021, pp. 355–362.
- [4] R. Brayton and A. Mishchenko, "Abc: An academic industrial-strength verification tool," in *Computer Aided Verification*, T. Touili, B. Cook, and P. Jackson, Eds. Berlin, Heidelberg: Springer Berlin Heidelberg, 2010, pp. 24–40.
- [5] H. S. STONE, "Chapter vi - universal logic modules," in *Recent Developments in Switching Theory*, A. Mukhopadhyay, Ed. Academic Press, 1971, pp. 229–254. [Online]. Available: <https://www.sciencedirect.com/science/article/pii/B9780125098502500117>
- [6] X. Chen and X. Wu, "Derivation of universal logic modules by algebraic means," *IEE Proceedings E (Computers and Digital Techniques)*, vol. 128, pp. 205–211(6), September 1981.
- [7] F. Preparata, "On the design of universal boolean functions," *IEEE Transactions on Computers*, vol. C-20, no. 4, pp. 418–423, 1971.
- [8] S. Yau and C. Tang, "Universal logic modules and their applications," *IEEE Transactions on Computers*, vol. C-19, no. 2, pp. 141–149, 1970.
- [9] J. H. Anderson, Q. Wang, and C. Ravishankar, "Raising fpga logic density through synthesis-inspired architecture," *IEEE Transactions on Very Large Scale Integration (VLSI) Systems*, vol. 20, no. 3, pp. 537–550, 2012.
- [10] J. Cong and Y.-Y. Hwang, "Boolean matching for lut-based logic blocks with applications to architecture evaluation and technology mapping," *IEEE Transactions on Computer-Aided Design of Integrated Circuits and Systems*, vol. 20, no. 9, pp. 1077–1090, 2001.
- [11] A. C. Ling, D. P. Singh, and S. D. Brown, "Fpga plb architecture evaluation and area optimization techniques using boolean satisfiability," *IEEE Transactions on Computer-Aided Design of Integrated Circuits and Systems*, vol. 26, no. 7, pp. 1196–1210, 2007.
- [12] Y. Okamoto, Y. Ichinomiya, M. Amagasaki, M. Iida, and T. Sueyoshi, "Cogre: A configuration memory reduced reconfigurable logic cell architecture for area minimization," in *2010 International Conference on Field Programmable Logic and Applications*. IEEE, 2010, pp. 304–309.
- [13] I. Ahmadpour, B. Khaleghi, and H. Asadi, "An efficient reconfigurable architecture by characterizing most frequent logic functions," in *2015 25th International Conference on Field Programmable Logic and Applications (FPL)*. IEEE, 2015, pp. 1–6.
- [14] A. Kennings, K. Vorwerk, A. Kundu, V. Pevzner, and A. Fox, "Fpga technology mapping with encoded libraries and staged priority cuts," *ACM Transactions on Reconfigurable Technology and Systems (TRETS)*, vol. 4, no. 4, pp. 1–17, 2011.
- [15] D. Lewis, G. Chiu, J. Chromczak, D. Galloway, B. Gamsa, V. Manoharajah, I. Milton, T. Vanderhoek, and J. Van Dyken, "The stratix™ 10 highly pipelined fpga architecture," in *Proceedings of the 2016 ACM/SIGDA International Symposium on Field-Programmable Gate Arrays*, 2016, pp. 159–168.
- [16] B. Gaide, D. Gaitonde, C. Ravishankar, and T. Bauer, "Xilinx adaptive compute acceleration platform: Versaltm architecture," in *Proceedings of the 2019 ACM/SIGDA International Symposium on Field-Programmable Gate Arrays*, 2019, pp. 84–93.
- [17] X. Zhou, L. Wang, and A. Mishchenko, "Fast exact npn classification by co-designing canonical form and its computation algorithm," *IEEE Transactions on Computers*, vol. 69, no. 9, pp. 1293–1307, 2020.
- [18] A. Mishchenko, R. Brayton, W. Feng, and J. Greene, "Technology mapping into general programmable cells," in *Proceedings of the 2015 ACM/SIGDA International Symposium on Field-Programmable Gate Arrays*, 2015, pp. 70–73.
- [19] M. Janota, W. Klieber, J. Marques-Silva, and E. Clarke, "Solving qbf with counterexample guided refinement," *Artificial Intelligence*, vol. 234, pp. 1–25, 2016.
- [20] J. Bergstra, D. Yamins, and D. Cox, "Making a science of model search: Hyperparameter optimization in hundreds of dimensions for vision architectures," in *International conference on machine learning*. PMLR, 2013, pp. 115–123.
- [21] A. Mishchenko, S. Cho, S. Chatterjee, and R. Brayton, "Combinational and sequential mapping with priority cuts," in *2007 IEEE/ACM International Conference on Computer-Aided Design*. IEEE, 2007, pp. 354–361.
- [22] A. Mishchenko and R. Brayton, "Faster logic manipulation for large designs," in *Proc. IWLS*, vol. 13, 2013.
- [23] A. Mishchenko, R. Brayton, J.-H. R. Jiang, and S. Jang, "Scalable don't-care-based logic optimization and resynthesis," *ACM Transactions on Reconfigurable Technology and Systems (TRETS)*, vol. 4, no. 4, pp. 1–23, 2011.
- [24] S. Yazdanshenas and V. Betz, "Coffe 2: Automatic modelling and optimization of complex and heterogeneous fpga architectures," *ACM Trans. Reconfigurable Technol. Syst.*, vol. 12, no. 1, jan 2019. [Online]. Available: <https://doi.org/10.1145/3301298>